Ayadualin, a novel RGD peptide with dual antihemostatic activities from the sand fly *Lutzomyia ayacuchensis*, a vector of Andean-type cutaneous leishmaniasis

Hirotomo Kato[a] *, Eduardo A. Gomez[b], Megumi Fujita[c], Yuka Ishimaru[c], Hiroshi Uezato[d], Tatsuyuki Mimori[e], Hiroyuki Iwata[c], Yoshihisa Hashiguchi[f,g,h]

[a]Laboratory of Parasitology, Department of Disease Control, Graduate School of Veterinary Medicine, Hokkaido University, Sapporo, Japan

[b]Departamento de Medicina Tropical, Facultad de Medicina, Universidad Catolica de Guayaquil, Ecuador

[c]Laboratory of Veterinary Hygiene, Faculty of Agriculture, Yamaguchi University, Yamaguchi, Japan

[d]Department of Dermatology, Faculty of Medicine, University of the Ryukyus, Okinawa, Japan

[e]Department of Microbiology, Faculty of Life Sciences, Graduate School of Health Sciences, Kumamoto University, Kumamoto, Japan

[f]Department of Parasitology, Kochi Medical School, Kochi University, Kochi, Japan

[g]Centro de Biomedicina, Universidad Central del Ecuador, Quito, Ecuador

[h]Prometeo, Secretaría Nacional de Educacion Superior, Ciencia, Tecnologia e Innovacion (SENESCYT), Ecuador

*Corresponding author. Tel. & Fax: +81-11-706-5196. *E-mail address*: hkato@vetmed.hokudai.ac.jp (H. Kato)

1. Introduction

Hematophagous insects have evolved a wide set of pharmacologically active molecules to counteract host hemostatic processes [1-3]. When probing in the host skin before blood feeding, they inject saliva, a cocktail of bioactive agents, containing anticoagulants, vasodilators, and inhibitors of platelet aggregation [1,2,4-6]. Other salivary molecules almost certainly involved in the feeding process include anti-inflammatory and immunosuppressive molecules [1,2,4-6]. Since hematophagous arthropods have evolved their feeding strategies independently, each species has developed unique pharmacologically active agents in their saliva to overcome host hemostatic defenses [1,3,5].

Phlebotomine sand flies are hematophagous insects of the family Psychodidae in the order Diptera, and some of them transmit *Leishmania* protozoa, the causative agent of leishmaniasis [7,8]. In addition to the antihemostatic activity, sand fly saliva exacerbates the infection of *Leishmania* parasites in mammalian hosts [9-11]. To date, the profiles of salivary components have been defined in 6 Old World *Phlebotomus* species; *Phlebotomus (P.) papatasi*, *P. ariasi*, *P. perniciosus*, *P. argentipes*, *P. duboscqi*, *P. arabicus,* and *P. orientalis* [12-17] and 3 *Lutzomyia* species; *Lutzomyia (Lu.) longipalpis*, *Lu. ayacuchensis*, and *Lu. intermedia* [18-21]. In the salivary transcriptome analysis of *Lu. ayacuchensis*, a proven vector of *L. (Leishmania) mexicana* in Ecuadorian Andes [22-24] and *L. (Viannia) peruviana* in Peruvian Andes [24,25], a peptide containing an RGD (Arg-Gly-Asp) sequence flanked by cysteine residues in the C-terminal end was identified as the most abundant transcript. A homologous protein has been identified in the salivary gland transcriptome of *Lu. longipalpis* (LuloRGD); however, the function remains to be characterized [18].

The RGD sequence present in adhesive proteins is recognized by several integrins, and binding of fibrinogen to integrin $\alpha_{IIb}\beta_3$ (glycoprotein GPIIb-IIIa) expressed on activated platelets via the RGD sequences is a crucial mechanism for platelet aggregation [26]. Thus, molecules containing RGD sequences have the potential to inhibit platelet aggregation by interfering with the binding of platelets to fibrinogen. The natural RGD-containing peptide, disintegrin, is a family of cysteine-rich peptides containing RGD motifs, discovered originally in snake venoms and later in saliva of hematophagous animals such as leeches and ticks [27-29]. Disintegrins present their RGD sequences to integrins by forming a characteristic disulfide bond-stabilized loop, the formation of which is essential for their activity, and competitively interfere with the binding between fibrinogen and integrins resulting in inhibition of platelet aggregation [27-29]. In insects, this family of proteins has been found solely in the salivary glands of the horsefly *Tabanus yao* [29,30]. On the other hand, a short RGD-containing peptide was identified from *Lu. ayacuchensis* and it has an RGD sequence in the C-terminal end, which differs from disintegrin family proteins. Additionally, it has only two cysteine residues located on both sides of the C-terminal RGD sequence, which is uncommon in disintegrins. In the present study, a recombinant protein of the short RGD-containing peptide from *Lu. ayacuchensis* salivary glands, designated ayadualin, was prepared, and its biological activity was characterized.

2. Materials and methods

2.1.Sequence analysis

The sequences were aligned with CLUSTAL W software [31] and examined using the program MEGA (Molecular Evolutionary Genetics Analysis) version 5.1 [32]. A phylogenetic tree by the neighbor-joining method was constructed with the distance algorithms available in the MEGA package. Bootstrap values were determined on 1,000 replicates of the data sets.

2.2. Production of recombinant proteins

A DNA fragment encoding full length of mature ayadualin was amplified and inserted into the *Eco*RI site of N-terminal thioredoxin (Trx)-hexahistidine (His)-tagged fusion plasmid vector, pET-32b(+) (Novagen, Drams, Germany). The *Eco*RI adaptor-ligated primers used for PCR amplification were Eco-LayS45-S (5'-ccgaattcGATGCCAAGGGAAAGCGTAAA-3') and Eco-LayS45-R (5'-ccgaattcTTACTAGCAGTCTCCTCTAC-3'). The fragment encoding ayadualin ΔRGD lacking a C-terminal RGD sequence were amplified with Eco-LayS45-S and Eco-LayS45-RGD(-)-R (5'-ccgaattcCTAACAGGGATATGGATTATGAC-3') primers, and the fragment encoding an ayadualin CS mutant, in which two cysteine residues franking a C-terminal RGD sequence were substituted by serine residues, was amplified with Eco-LayS45-S and Eco-LayS45 (C→S)-R (5'-ccgaattcCTAGCTGTCTCCTCTAGAGGGAT-3') primers. *Escherichia coli* (*E. coli*) BL21 cells were transformed with the recombinant plasmid and grown in Luria-Bertani (LB) medium containing ampicillin (50 μg/ml). Production of Trx-His-tagged recombinant ayadualins was induced by addition of isopropyl β-D-thiogalactoside

(IPTG) to a final concentration of 0.5 mM. BL21 cells suspended in binding buffer (20 mM sodium phosphate, 500 mM NaCl, 20 mM imidazol, pH 7.4) were sonicated, and recombinant protein was purified from the soluble fraction using His GraviTrap (GE Healthcare, Buckinghamshire, UK) and finally dialyzed against phosphate-buffered saline (PBS). Trx-His-tag protein only was expressed and purified for use as a control.

2.3. Sodium dodecyl sulfate polyacrylamide gel electrophoresis and immunoblotting

The samples were treated with 2x SDS sample buffer [125 mM Tris-HCl (pH6.8), 4.5% SDS, 20% glycerol, 0.01% bromophenol blue and 10% 2-mercaptoethanol] and analyzed in a 15% polyacrylamide gel. The molecular weight of recombinant proteins was estimated using Precision Plus Protein Standards (Bio-Rad Laboratories, Hercules, CA). After electrophoresis, the gel was stained with coomassie brilliant blue.

For the immunoblotting, the proteins in the gel were transferred to polyvinylidene difluoride (PVDF) membranes (Millipore, Bedford, MA). After blocking with 5% skim milk in PBS for 1 hr at room temperature, the membrane was incubated with a mouse anti-His antibody (GE Healthcare) overnight at 4˚C. After washing three times with PBS containing 0.05% Tween 20 (PBS-T), the membrane was further incubated with alkaline phosphatase (AP)-conjugated goat anti-mouse immunoglobulin (Zymed laboratories, San Francisco, CA) for 1 hr at room temperature. After three washes with PBS-T, the blots were developed by addition of substrate (Alkaline Phosphatase Conjugate Substrate Kit; Bio-Rad Laboratories) and visualized.

2.4. Platelet aggregation assay

Blood was collected from a healthy human volunteer by vein puncture in accordance

with the approval of the research ethics committee of Hokkaido University (license number: 26-2), placed in sodium citrate and centrifuged at 100 x g for 15 min to obtain platelet-rich plasma (PRP). Platelet aggregation was measured by using a microplate method as described previously [33]. Briefly, 100 µl of PRP was mixed with 30 µl of ayadualin, ΔRGD, CS mutant or Trx-His-tag protein with a final concentration of 20, 10, 5, 2.5, 1.25 or 0.625 µM, and platelet aggregation was induced immediately by addition of 20 µl of ADP (final concentration, 5 µM) (Arkray, Kyoto, Japan) or type I collagen (final concentration, 10 µg/ml) (Arkray). The mixture was incubated at 37˚C for 15 min in a shaking incubator (SI-300; AS ONE, Osaka, Japan), and platelet aggregation was measured by determining the change in light transmission at a wavelength of 630 nm using a microplate reader (iMark: Bio-Rad Laboratories). Data were analyzed and the IC_{50} values were determined by non-linear regression (curve-fitting) using GraphPad Prism version 6.05. (GraphPad Software, Inc., CA).

2.5. Fibrinogen/integrin $\alpha_{IIb}\beta_3$ (GPIIb/IIIa) Enzyme-linked Immunosorbent Assay (ELISA)

Fibrinogen/integrin $\alpha_{IIb}\beta_3$ (GPIIb/IIIa) ELISA was performed as described previously [34] with some modifications. A microtiter plate (MaxiSorp immuno plate; NUNC, Roskilde, Denmark) was coated with a solution of fibrinogen (20 µg/ml) (Sigma, St. Louis, MO) in Tris-buffered saline [TBS; 40 mM Tris-HCl (pH 7.4) and 150 mM NaCl] overnight at 4˚C. The wells were washed with PBS-T, and blocked with a solution of 0.5% bovine serum albumin (BSA) in TCTS buffer [20 mM Tris-HCl (pH7.4), 2 mM $CaCl_2$, 0.05 % Tween 20 and 120 mM NaCl] for 2 hrs at room temperature. After three washes, serially-diluted recombinant proteins (ayadualin,

ΔRGD, a CS mutant or Trx-His-tag protein) and purified human integrin $\alpha_{IIb}\beta_3$ (GPIIb/IIIa) (20 μg/ml) (Enzyme Research Laboratories, South Bend, IN) were added. After incubation for 1 hr at 37˚C, the wells were washed three times with PBS-T, and a mouse anti-human CD41 (GPIIb) monoclonal antibody (Exbio, Praha, Czech Republic) was added. Following 1 hr-incubation at 37˚C and three washes, the wells were further incubated with horseradish peroxidase (HRP)-conjugated goat anti-mouse IgG (BD Biosciences, San Diego, CA) for 1 hr at 37˚C. After three washes with PBS-T, the wells were developed by addition of substrate (TMB Peroxidase EIA Substrate Kit; Bio-Rad Laboratories). The reaction was stopped by addition of 1N H_2SO_4 and the absorbance at 450 nm was measured.

2.6. Effect of ayadualin on plasma coagulation

The effect of ayadualin on plasma coagulation was tested by measuring the prothrombin time (PT) and activated partial thromboplastin time (APTT). Forty-five microliters of citrated normal human plasma was mixed with 5 μl of ayadualin, ΔRGD or Trx-His-tag protein with a final concentration of 30, 15 or 7.5 μM and incubated for 3 min at 37˚C. Plasma coagulation was activated for 3 min at 37˚C with 100 μl of PT reagent (thromboplastin from rabbit brain; Sysmex, Hyogo, Japan) for the PT assay, or for 1 min at 37˚C with 50 μl of APTT reagent (synthetic phospholipid; Sysmex) followed by 50 μl of 0.02 M $CaCl_2$ for 2 min at 37˚C for the APTT assay. The clot formation was measured using a CA-50 coagulometer (Sysmex).

2.7. Effect of ayadualin on the intrinsic pathway of blood coagulation

The effect of ayadualin on the intrinsic coagulation pathway was assessed based on

the generation of activated coagulation factors (kallikrein, FIXa, FXa, and FXIIa). Citrated human plasma was treated with acid to inactivate plasma serine protease inhibitors, and diluted with 1:9 in 20 mM Tris-HCl, pH7.4, 150 mM NaCl, 2 mM EDTA, and 0.2% polyethylene glycol 8000 (PEG8000) [35]. Fifty microliters of acid-treated human plasma was pre-incubated for 5 min at 37˚C with 15 μl of serially-diluted ayadualin. The mixture was activated by adding 5 μl of APTT reagent for 10 min at 37˚C followed by 5 μl of 0.02 M $CaCl_2$. After 1 min at 37˚C, 25 μl of chromogenic substrate was added to a final concentration of 0.5 mM [36,37], and the amidolytic activity of the enzyme generated was determined at a wavelength of 405 nm using a microplate reader (iMark: Bio-Rad Laboratories). The chromogenic substrates used were as follows: SPECTROZYME FIXa (American Diagnostica, Greenwich, CT, USA) for FIXa, SPECTROZYME FXa (American Diagnostica) for FXa, SPECTROZYME FXIIa (American Diagnostica) for FXIIa, and SPECTROZYME P.Kal (American Diagnostica) for the kallikrein assay. Soybean trypsin inhibitor, an inhibitor of plasma kallikrein (SBTI; Wako Pure Chemical Industries, Osaka, Japan) was added to the FXIIa assay to a final concentration of 20 nM [37]. Data were analyzed and the IC_{50} values were determined by non-linear regression (curve-fitting) using GraphPad Prism version 6.05. (GraphPad Software, Inc., CA).

2.8. Effect of ayadualin on FXII

The effect of ayadualin on FXII activation was assessed as follows: human FXII (final concentration, 0.2 μM) (Haematologic Technologies Inc., Essex Junction, VT, USA) was pre-incubated with serially diluted ayadualin for 5 min at 37˚C in the presence of $ZnCl_2$ (0.5 mM), and activated by addition of 5 μl of APTT reagent

(Sysmex) for 5 min at 37˚C. The effect of ayadualin on the enzymatic activity of FXIIa was assessed as follows: human FXII (0.2 μM) (Haematologic Technologies Inc.) was activated with 5 μl of APTT reagent (Sysmex) for 5 min at 37˚C in the presence of $ZnCl_2$ (0.5 mM), and then incubated with serially diluted ayadualin for 5 min at 37˚C. The activity of FXIIa was measured using the chromogenic substrate SPECTROZYME FXIIa (American Diagnostica).

2.9. *Effect of ayadualin on FXa and kallikrein activity in FXII-deficient plasma*

The effect of ayadualin on FXa and kallikrein activity was assessed using FXII-deficient plasma. Acid-treated diluted FXII-deficient plasma was pre-incubated with ayadualin or Trx-His-tag protein (final concentration, 4 μM) for 5 min at 37˚C, and activated by addition of purified FXIIa (final concentration, 50 ng/ml) (Hyphen Biomed, Neuville sur Oise, France) and 5 μl of 0.02 M $CaCl_2$. After 5 min at 37˚C, 25 μl of chromogenic substrate was added, and the amidolytic activity of FXa and kallikrein was determined at a wavelength of 405 nm using a microplate reader (iMark: Bio-Rad Laboratories).

3. Results

3.1.Sequence analysis of the RGD-containing peptide, ayadualin

A short peptide containing an RGD (Arg-Gly-Asp) sequence flanked by cysteine residues in the C-terminal end was identified as the most abundant transcript in the *Lu. ayacuchensis* salivary glands [20]. This peptide, named ayadualin, (GenBank accession number: AK416785) coded for 67 amino acids containing a 20 amino acid signal peptide with a predicted molecular mass of 5.3 kDa in the mature form (Fig. 1A). The homologous proteins identified so far are salivary RGD-containing peptides from *Lu. longipalpis* (LuloRGD) at 52% identity, and the SP13 protein family from *Lu. intermedia*, Linb-1 and Linb-2, at 32% and 36% identities, respectively (Fig. 1B). No cysteine residue is found in LuloRGD, while Linb-1 and Linb-2 each contain two cysteines at their C-terminal end, one of which is at the corresponding position to that of ayadualin (Fig. 1B). The sand fly RGD peptides were not homologous to disintegrin family proteins, which are well-characterized RGD-containing peptides originally identified in snake venom that function as inhibitors of platelet aggregation [26] (Fig. S1).

3.2. Production and purification of recombinant ayadualins

To characterize the biological function of ayadualin, the recombinant protein was expressed in *E. coli* as a Trx-His-tagged fusion protein and purified from the soluble fraction of the *E. coli* lysate. Ayadualin ΔRGD lacking the RGD sequence was prepared to define the function of the RGD sequence of this protein, and a CS mutant, in which two cysteines flanking the RGD sequence were substituted by serine residues, was prepared to determine the importance of a disulfide bond formed by the two cysteine

residues (Fig. S2). Trx-His-tagged ayadualin, ΔRGD and the CS mutant had a molecular mass of approximately 25 kDa based on polyacrylamide gel electrophoresis (Fig. 2) and reacted to an anti-His antibody in immunoblotting.

3.3. Ayadualin inhibits platelet aggregation by inhibiting the binding of integrin $\alpha_{IIb}\beta_3$ to fibrinogen

The effect of ayadualin on platelet aggregation was examined. Both collagen and ADP-induced platelet aggregations were inhibited by ayadualin in a dose-dependent manner with IC_{50} values at 8.37 μM and 5.66 μM, respectively (Fig. 3), indicating that salivary ayadualin acts as a platelet aggregation inhibitor during the blood-feeding process of *Lu. ayacuchensis*. On the other hand, such inhibition was not observed by addition of ΔRGD, indicating that the RGD sequence is essential for the inhibitory effect against platelet aggregation. In addition, substitution of cysteine residues flanking the RGD sequence to serine residues (CS mutant) abrogated its inhibitory effect, strongly suggesting that the disulfide bond structure of ayadualin is critical to its antiplatelet action.

To determine if inhibitory activity of ayadualin is mediated by the interference of the binding of integrin $\alpha_{IIb}\beta_3$ to fibrinogen, a fibrinogen/integrin $\alpha_{IIb}\beta_3$ ELISA was performed in the presence of recombinant ayadualin, ΔRGD or the CS mutant. As shown in Fig. 4, ayadualin inhibited binding of integrin $\alpha_{IIb}\beta_3$ to fibrinogen in a dose-dependent manner (IC_{50} 0.15 μM). On the other hand, both ΔRGD and the CS mutant lost the inhibitory effect (Fig. 4), corresponding to the results of their antiplatelet activities. These results indicate that interfering with the binding between integrin $\alpha_{IIb}\beta_3$ and fibrinogen is a crucial mechanism for ayadualin to inhibit platelet aggregation via

the RGD sequence.

3.4. Ayadualin inhibits activation of the contact phase of the intrinsic blood coagulation pathway

The effect of ayadualin on plasma coagulation was examined by measuring PT and APTT. In the presence of ayadualin, APTT, but not PT, was prolonged in a dose-dependent manner (Fig. 5). Interestingly, ΔRGD also prolonged APTT with equal activity to ayadualin (Fig. 5). This result indicates that ayadualin inhibits the intrinsic blood coagulation pathway independently of the RGD sequence. To characterize the mechanism involved in the anticoagulation activity of ayadualin, an amidolytic assay was performed using chromogenic substrates specific to kallikrein, FXIIa, FIXa and FXa. Enzymatic activities of kallikrein, FXIIa, FIXa and FXa were markedly inhibited in the presence of ayadualin, and above all, FXIIa activity was the most affected (Fig. 6A-D), suggesting that the primary target of ayadualin is FXII. The IC_{50} value of ayadualin was estimated to be 2.08 μM for kallikrein, 0.64 μM for FXIIa, 2.13 μM for FIXa and 1.71 μM for FXa. To determine whether ayadualin inhibits the activation of FXII or enzymatic activity of FXIIa, FXII was treated with ayadualin before or after the activation, and then the enzymatic activity of FXIIa was measured. As shown in Fig. 7, pre-treatment of FXII with ayadualin inhibited FXIIa activity in a dose-dependent manner, while the generated FXIIa was not affected by ayadualin, indicating that ayadualin inhibits the activation of FXII, but not the enzymatic activity of FXIIa.

To confirm the direct effect of ayadualin on FXa and kallikrein, FXII-deficient plasma was activated by FXIIa in the presence of ayadualin, and production of FXa and kallikrein was examined. The inhibition of ayadualin on FXa and kallikrein production

was not observed in the absence of FXII, indicating that the primary target of ayadualin is FXII but not downstream pathway of the coagulation cascade such as FX and kallikrein (Fig. S3).

4. Discussion

Ayadualin was identified as the most abundant transcript in salivary glands of *Lu. ayacuchensis* [20]. The peptide shared homology with salivary RGD peptides from *Lu. longipalpis* (LuloRGD) and *Lu. intermedia* (Linb-1 and Linb-2) [18,19,21], but not with other proteins, suggesting that these peptides are unique to *Lutzomyia* species. Although these peptides are expected to function as platelet aggregation inhibitors via their RGD sequences, their functions have not been characterized. In this study, a recombinant ayadualin was produced, and its biological activity was characterized. Ayadualin interfered with the binding of integrin $\alpha_{IIb}\beta_3$ to fibrinogen, resulting in the inhibition of platelet aggregation. The RGD sequence in the C-terminal end and cysteine residues located on both sides of the RGD sequence were essential for the inhibitory effect. In addition, ayadualin efficiently inhibited intrinsic blood coagulation by targeting the activation of FXII independently on the RGD sequence.

The RGD sequence present in matrix proteins is known to be the binding site for integrins [26]. The natural RGD-containing peptides, disintegrins, identified in snake venoms, and the salivary glands of leeches, ticks, and horseflies, were shown to inhibit platelet aggregation by interfering with the binding of integrin $\alpha_{IIb}\beta_3$ on platelets to fibrinogen [27-29]. Functional analysis of ayadualin showed that the peptide inhibited both collagen and ADP-induced platelet aggregation, and the inhibition depended on the C-terminal RGD sequence and disulfide bond structure located on both sides of the RGD sequence. The relatively weaker inhibitory effect of ayadualin observed in the collagen-induced platelet aggregation suggested the involvement of several molecules, including integrin $\alpha_{IIb}\beta_3$, in the primary platelet aggregation induced by collagen. Our result demonstrated that ayadualin required a higher concentration, at the micromolar

level (IC_{50} 5.66 μM), for the inhibition of ADP-induced platelet aggregation than that reported in disintegrins (IC_{50} ~150-300 nM) [28,29]. Similarly, the inhibitory activity of the binding between integrin $\alpha_{IIb}\beta_3$ and fibrinogen was lower in ayadualin (IC_{50} 0.15 μM) when compared to that of disintegrins (IC_{50} ~1.5-5 nM) [28,29]. The loop structure characterized in disintegrins may be required to express maximum binding affinity of the RGD sequence to integrins, although ayadualin is expected to form a disulfide bond structure to present the RGD sequence. However, the activity between ayadualin and other disintegrins cannot be compared simply because disintegrins have been prepared by several methods: purified from salivary protein, and produced by insect cells or bacteria system. Preparation of recombinant protein by *E. coli* may cause an inappropriate folding, resulting in lower activity, as reported in the minor amounts of recombinant ornatin, a disintegrin identified from a leech. [38]. Consistent with previous studies using reducing agents-treated disintegrins [39,40] and synthetic cyclic and linear RGD peptides [41-43], a disulfide bond structure composed of two cysteine residues flanking the RGD sequence was essential for the antiplatelet action of ayadualin since substitution of the cysteines to serine residues abrogated the activity. Different from ayadualin, cysteine residues were not found in the previously reported RGD-containing peptide (LuloRGD) from *Lu. longipalpis* saliva [18,19], strongly suggesting that the peptide has no antiplatelet activity. Another motif for platelet fibrinogen receptor, the PXXXDX sequence [42], was found in ayadualin at amino acid 46-51 of the immature protein (Fig. 1A). However, little inhibition (<10%) of binding between integrin $\alpha_{IIb}\beta_3$ and fibrinogen by ΔRGD was observed even at a higher concentration (~5 μM), and deletion of the RGD sequence was enough to abrogate the antiplatelet activity, suggesting that the PXXXDX sequence is not essential for the

biological function of ayadualin.

In addition to its antiplatelet action, ayadualin efficiently inhibited intrinsic blood coagulation by targeting the activation of FXII independently on the RGD sequence. The intrinsic pathway is initiated by the binding of FXII to negatively charged surfaces, leading to the conversion of the inactive FXII into the active serine protease FXIIa. FXIIa converts prekallikrein into kallikrein and FXI into FXIa, followed by activation of FIX and then FX to generate FXa [36,44]. Measuring the enzymatic activity of coagulation factors using chromogenic substrates, FXIIa activity was markedly inhibited by ayadualin in a dose-dependent manner. Although ayadualin also inhibited kallikrein, FIXa and FXa activities, the inhibition was lower than that of FXIIa. These results strongly suggested that the primary target of ayadualin is FXII, and the downstream pathway of the intrinsic coagulation cascade such as activation of kallikrein, FIX and FX, was affected by impaired FXIIa activity. Inhibition of the activation process of FXII, but not the enzymatic activity of FXIIa, by ayadualin was shown by use of a recombinant FXII. In addition, the inhibition of ayadualin on the downstream pathway was not observed in the absence of FXII. Therefore, ayadualin works as an anticoagulant by targeting the contact phase initiated by FXII activation in the blood coagulation cascade during the blood feeding of *Lu. ayacuchensis*.

To date, not many salivary proteins have been functionally characterized in sand flies because of their unique structure. Salivary hyaluronidase (a hypothetical blood meal acquisition facilitator), adenosine deaminase (a hypothetical pain reliever), and apyrase (an ADP-induced platelet aggregation inhibitor) were characterized in several sand fly species based on the biological function of their homologues from mammals and other insects [16,33,45-47]. On the other hand, only a few structurally unique

proteins identified from sand fly saliva have been functionally characterized; maxadillan as a strong vasodilator [48] and lufaxin as a factor Xa inhibitor [49], both from *Lu. longipalpis*. This unique form of the RGD peptide is found only in the saliva of *Lutzomyia* species [18-21], and ayadualin is the first salivary protein from sand flies to be found to have a dual inhibitory effect on hemostasis. In addition, this peptide inhibits platelet aggregation by a different mechanism from apyrase, the only known antiplatelet component from sand fly saliva, and is the first inhibitor of the intrinsic coagulation pathway from sand flies.

5. Conclusion

In the present study, functional characterization of a recombinant salivary RGD peptide from *Lu. ayacuchensis*, named ayadualin, revealed that ayadualin affects host hemostasis by dual mechanisms; inhibition of platelet aggregation and an anticoagulant action in the contact phase. Therefore, this peptide is considered to play an important role in the blood feeding process of *Lu. ayacuchensis*. Because of its unique structure, further structural analysis of the peptide may help understanding of the inhibitory mechanism of FXII activity. In addition, ayadualin has potential as a pharmacological substance, as well as a reagent for a wide variety of research purposes.

Conflicts of interest

The authors have declared that there is no conflict of interest.

Author contributions

H.K. designed the study, performed experiments, and drafted the manuscript; E.A.G. contributed to the sample preparation; M.F., Y.I. and H.I. performed experiments; H.U. and T.M. analyzed the data and contributed to the statistics; Y.H. edited the manuscript

Acknowledgements

This study was supported in part by Grants-in-aid for Scientific Research from Japan Science and Technology Agency (JST), A-STEP feasibility study program (No. AS242Z00081Q), and the Ministry of Education, Science, Culture and Sports of Japan (No. 23580424).

References

[1] J.M.C. Ribeiro, Blood-feeding arthropods: live syringes or invertebrate pharmacologists? Infect. Agents. 4 (1995) 143-152.

[2] J.M.C. Ribeiro, I.M.B. Francischetti, Role of arthropod saliva in blood feeding: sialome and post-sialome perspectives. Annu. Rev. Entomol. 48 (2003) 73-88.

[3] A. Fontaine, I. Diouf, N. Bakkali, D. Missé, F. Pagès, T. Fusai, C. Rogier, L. Almeras, Implication of haematophagous arthropod salivary proteins in host-vector interactions. Parasit. Vectors. 4 (2011) 187.

[4] J.G. Valenzuela, Blood-Feeding Arthropod Salivary Glands and Saliva. In: W.C. Marquardt, W.C. Black, J.E. Freier, H.H. Hagedorn, J. Hemingway, S. Higgs, A.A. James, B. Kondratieff, C.G. Moore (Ed.). Biology of Disease Vectors. Second edition. Elsevier, San Diego CA: 2004, p377-386.

[5] D.E.Champagne, Antihemostatic molecules from saliva of blood-feeding arthropods. Pathophysiol. Haemost. Thromb. 34 (2005) 221-227.

[6] J.F. Andersen, N.P. Gudderra, I.M.B. Francischetti, J.M.C. Ribeiro, The role of salivary lipocalins in blood feeding by *Rhodnius prolixus*. Arch. Insect Biochem. Physiol. 58 (2005) 97-105.

[7] L.E. Munstermann, Phlebotomine sand flies, the Psychodidae. In: W.C. Marquardt, W.C. Black, J.E. Freier, H.H. Hagedorn, J. Hemingway, S. Higgs, A.A. James, B. Kondratieff, C.G. Moore (Ed.). Biology of Disease Vectors. Second edition. Elsevier, San Diego CA: 2004; 141-151.

[8] H. Kato, E.A. Gomez, A.G. Cáceres, H. Uezato, T. Mimori, Y. Hashiguchi, Molecular epidemiology for vector research on leishmaniasis. Int. J. Environ. Res. Public Health, 7 (2010) 814-826.

[9] R.G. Titus, J.M.C. Ribeiro, Salivary gland lysates from the sand fly *Lutzomyia longipalpis* enhance *Leishmania* infectivity. Science. 239 (1988) 1306-1308.

[10] C.M. Theodos, J.M.C. Ribeiro, R.G. Titus, Analysis of enhancing effect of sand fly saliva on *Leishmania* infection in mice. Infect. Immun, 59 (1991) 1592-1598.

[11] H.C. Lima, R.G. Titus, Effects of sand fly vector saliva on development of cutaneous lesions and the immune response to *Leishmania braziliensis* in BALB/c mice. Infect. Immun. 64 (1996) 5442-5445.

[12] J.G. Valenzuela, Y. Belkaid, M.K. Garfield, S. Mendez, S. Kamhawi, E.D. Rowton, D.L. Sacks, J.M.C. Ribeiro Toward a defined anti-*Leishmania* vaccine targeting vector antigens: characterization of a protective salivary protein. J. Exp. Med. 194 (2001) 331-342.

[13] F. Oliveira, S. Kamhawi, A.E. Seitz, V.M. Pham, P.M. Guigal, L. Fischer, J. Ward, J.G. Valenzuela, From transcriptome to immunome: identification of DTH inducing proteins from a *Phlebotomus ariasi* salivary gland cDNA library. Vaccine. 24 (2006) 374-390.

[14] J.M. Anderson, F. Oliveira, S. Kamhawi, B.J. Mans, D. Reynoso, A.E. Seitz, P. Lawyer, M. Garfield, M. Pham, J.G. Valenzuela, Comparative salivary gland transcriptomics of sandfly vectors of visceral leishmaniasis. BMC Genomics. 7 (2006) 52.

[15] H. Kato, J.M. Anderson, S. Kamhawi, F. Oliveira, P.G. Lawyer, V.M. Pham, C.S. Sangare, S. Samake, I. Sissoko, M. Garfield, L. Sigutova, P. Volf, S. Doumbia, J.G. Valenzuela, High degree of conservancy among secreted salivary gland proteins from two geographically distant *Phlebotomus duboscqi* sandflies populations (Mali and Kenya). BMC Genomics. 7 (2006) 226.

[16] J. Hostomská, V. Volfová, J. Mu, M. Garfield, I. Rohousová, P. Volf, J.G. Valenzuela, R.C. Jochim, Analysis of salivary transcripts and antigens of the sand fly *Phlebotomus arabicus*. BMC Genomics. 10 (2009) 282.

[17] M. Vlkova, M. Sima, I. Rohousova, T. Kostalova, P. Sumova, V. Volfova, E.L. Jaske, K.D. Barbian, T. Gebre-Michael, A. Hailu, A. Warburg, J.M.C. Ribeiro, J.G. Valenzuela, R.C. Jochim, P. Volf, Comparative analysis of salivary gland transcriptomes of *Phlebotomus orientalis* sand flies from endemic and non-endemic foci of visceral leishmaniasis. PLoS Negl. Trop. Dis. 8 (2014) e2709.

[18] R. Charlab, J.G. Valenzuela, E.D. Rowton, J.M.C. Ribeiro, Toward an understanding of the biochemical and pharmacological complexity of the saliva of a hematophagous sand fly *Lutzomyia longipalpis*. Proc. Natl. Acad. Sci. U.S.A. 96 (1999) 15155-15160.

[19] J.G. Valenzuela, M. Garfield, E.D. Rowton, V.M. Pham, Identification of the most abundant secreted proteins from the salivary glands of the sand fly *Lutzomyia longipalpis*, vector of *Leishmania chagasi*. J. Exp. Biol. 207 (2004) 3717-3729.

[20] H. Kato, R.C. Jochim, E.A. Gomez, H. Uezato, T. Mimori, M. Korenaga, T. Sakurai, K. Katakura, J.G. Valenzuela, Y. Hashiguchi, Analysis of salivary gland transcripts of the sand fly *Lutzomyia ayacuchensis*, a vector of Andean-type cutaneous leishmaniasis. Infect. Genet. Evol. 13 (2013) 56-66.

[21] T.R. de Moura, F. Oliveira, M.W. Carneiro, J.C. Miranda, J. Clarêncio, M. Barral-Netto, C. Brodskyn, A. Barral, J.M.C. Ribeiro, J.G. Valenzuela, C.I. de Oliveira, Functional transcriptomics of wild-caught *Lutzomyia intermedia* salivary glands: identification of a protective salivary protein against *Leishmania braziliensis* infection. PLoS Negl. Trop. Dis. 7 (2013) e2242

[22] H. Takaoka, E.A. Gomez, J.B. Alexander, Y. Hashiguchi, Natural infections with *Leishmania* promastigotes in *Lutzomyia ayacuchensis* (Diptera: Psychodidae) in an Andean focus of Ecuador. J. Med. Entomol. 27 (1990) 701-702.

[23] H. Kato, H. Uezato, K. Katakura, M. Calvopiña, J.D. Marco, P.A. Barroso, E.A. Gomez, T. Mimori, M. Korenaga, H. Iwata, S. Nonaka, Y. Hashiguchi, Detection and identification of *Leishmania* species within naturally infected sand flies in the andean areas of Ecuador by a polymerase chain reaction. Am. J. Trop. Med. Hyg. 72 (2005) 87-93.

[24] H. Kato, A.G. Cáceres, E.A. Gomez, T. Mimori, H. Uezato, J.D. Marco, P.A. Barroso, H. Iwata, Y. Hashiguchi, Molecular mass screening to incriminate sand fly vectors of Andean-type cutaneous leishmaniasis in Ecuador and Peru. Am. J. Trop. Med. Hyg. 79 (2008) 719-721.

[25] A.G. Caceres, P. Villaseca, J.C. Dujardin, A.L. Bañuls, R. Inga, M. Lopez, M. Arana, D. Le Ray, J. Arevalo, Epidemiology of Andean cutaneous leishmaniasis: incrimination of *Lutzomyia ayacuchensis* (Diptera: Psychodidae) as a vector of *Leishmania* in geographically isolated, upland valleys of Peru. Am. J. Trop. Med. Hyg. 70 (2004) 607-612.

[26] R.O. Hynes, Integrins: versatility, modulation, and signaling in cell adhesion. Cell. 69 (1992) 11-25.

[27] C.P. Blobel, J.M. White, Structure, function and evolutionary relationship of proteins containing a disintegrin domain. Curr. Opin. Cell. Biol. 4 (1992) 760-765.

[28] I.M.B. Francischetti. Platelet aggregation inhibitors from hematophagous animals. Toxicon. 56 (2010) 1130-1144.

[29] T.C. Assumpcao, J.M.C. Ribeiro, I.M.B. Francischetti, Disintegrins from

hematophagous sources. Toxins. 4 (2012) 296-322.

[30] D. Ma, Y. Wang, H. Yang, J. Wu, S. An, L. Gao, X. Xu, R. Lai, Anti-thrombosis repertoire of blood-feeding horsefly salivary glands. Mol. Cell. Proteomics. 8 (2009) 2071-2079.

[31] J.D. Thompson, D.G. Higgins, T.J. Gibson, CLUSTAL W: improving the sensitivity of progressive multiple sequence alignment through sequence weighting, position-specific gap penalties and weight matrix choice. Nucleic Acids Res. 22 (1994) 4673-4680.

[32] K. Tamura, D. Peterson, N. Peterson, G. Stecher, M. Nei, S. Kumar, MEGA5: molecular evolutionary genetics analysis using maximum likelihood, evolutionary distance, and maximum parsimony methods. Mol. Biol. Evol. 28 (2011) 2731-2739.

[33] R. Hamasaki, H. Kato, Y. Terayama, H. Iwata, J.G. Valenzuela, Functional characterization of a salivary apyrase from the sand fly, *Phlebotomus duboscqi*, a vector of *Leishmania major*. J. Insect Physiol. 55 (2009) 1044-1049.

[34] J.L. Seymour, W.J. Henzel, B. Nevins, J.T. Stults, R.A. Lazarus, Decorsin. A potent glycoprotein IIb-IIIa antagonist and platelet aggregation inhibitor from the leech *Macrobdella decora*. J. Biol. Chem. 265 (1990) 10143-10147.

[35] N. Kato, S. Iwanaga, T. Okayama, H. Isawa, M. Yuda, Y. Chinzei, Identification and characterization of the plasma kallikrein-kinin system inhibitor, haemaphysalin, from hard tick, *Haemaphysalis longicornis*. Thromb. Haemost. 93 (2005) 359-367.

[36] Y. Decrem, G. Rath, V. Blasioli, P. Cauchie, S. Robert, J. Beaufays, J.M. Frère, O. Feron, J.M. Dogné, C. Dessy, L. Vanhamme, E. Godfroid, Ir-CPI, a coagulation contact phase inhibitor from the tick *Ixodes ricinus*, inhibits thrombus formation

without impairing hemostasis. J. Exp. Med. 206 (2009) 2381-2395.

[37] Y. Ishimaru, E.A. Gomez, F. Zhang, L. Martini-Robles, H. Iwata, T. Sakurai, K. Katakura, Y. Hashiguchi, H. Kato, Dimiconin, a novel coagulation inhibitor from the kissing bug, *Triatoma dimidiata*, a vector of Chagas disease. J. Exp. Biol. 215 (2012) 3597-3602.

[38] P. Mazur, M.S. Dennis, J.L. Seymour, R.A. Lazarus, Expression, purification, and characterization of recombinant ornatin E, a potent glycoprotein IIb-IIIa antagonist. Protein Expr. Purif. 4 (1993) 282-289.

[39] T.F. Huang, J.C. Holt, H. Lukasiewicz, S. Niewiarowski, Trigramin. A low molecular weight peptide inhibiting fibrinogen interaction with platelet receptors expressed on glycoprotein IIb-IIIa complex. J. Biol. Chem. 262 (1987) 16157-16163.

[40] Z.R. Gan, R.J. Gould, J.W. Jacobs, P.A. Friedman, M.A. Polokoff. Echistatin. A potent platelet aggregation inhibitor from the venom of the viper, *Echis carinatus*. J. Biol. Chem. 263 (1988) 19827-19832.

[41] X. Lu, J.J. Deadman, J.A. Williams, V.V. Kakkar, S. Rahman, Synthetic RGD peptides derived from the adhesive domains of snake-venom proteins: evaluation as inhibitors of platelet aggregation. Biochem. J. 296 (1993) 21-24.

[42] J. Katada, Y. Hayashi, Y. Sato, M. Muramatsu, Y. Takiguchi, T. Harada, T. Fujiyoshi, I. Uno, A novel peptide motif for platelet fibrinogen receptor recognition. J. Biol. Chem. 272 (1997) 7720-7726.

[43] Y. Hayashi, J. Katada, Y. Sato, K. Igarashi, Y. Takiguchi, T. Harada, M. Muramatsu, E. Yasuda, I. Uno, Discovery and structure--activity relationship studies of a novel and specific peptide motif, Pro-X-X-X-Asp-X, as a platelet fibrinogen receptor

antagonist. Bioorg. Med. Chem. 6 (1998) 355-364.

[44] J. Shan, M. Baguinon, L. Zheng, R. Krishnamoorthi, Expression, refolding, and activation of the catalytic domain of human blood coagulation factor XII. Protein Expr. Purif. 27 (2003) 143–149.

[45] R. Charlab, J.G. Valenzuela, J. Andersen, J.M.C. Ribeiro, The invertebrate growth factor/CECR1 subfamily of adenosine deaminase proteins. Gene. 267 (2001) 13-22.

[46] H. Kato, R.C. Jochim, P.G. Lawyer, J.G. Valenzuela, Identification and characterization of a salivary adenosine deaminase from the sand fly *Phlebotomus duboscqi*, the vector of *Leishmania major* in sub-Saharan Africa. J. Exp. Biol. 210 (2007) 733-740.

[47] J.G. Valenzuela, Y. Belkaid, E. Rowton, J.M.C. Ribeiro, The salivary apyrase of the blood-sucking sand fly *Phlebotomus papatasi* belongs to the novel *Cimex* family of apyrases. J. Exp. Biol. 204 (2001) 229-237.

[48] E.A. Lerner, C.B. Shoemaker, Maxadilan. Cloning and functional expression of the gene encoding this potent vasodilator peptide. J. Biol. Chem. 267 (1992) 1062-1066.

[49] N. Collin, T.C. Assumpção, D.M. Mizurini, D.C. Gilmore, A. Dutra-Oliveira, M. Kotsyfakis, A. Sá-Nunes, C. Teixeira, J.M.C. Ribeiro, R.Q. Monteiro, J.G. Valenzuela, I.M.B. Francischetti. Lufaxin, a novel factor Xa inhibitor from the salivary gland of the sand fly *Lutzomyia longipalpis* blocks protease-activated receptor 2 activation and inhibits inflammation and thrombosis *in vivo*. Arterioscler. Thromb. Vasc. Biol. 32 (2012) 2185-2198.

Figure Legends

Fig. 1. (A) Nucleotide and deduced amino acid sequences of an RGD-containing peptide, ayadualin, from *Lutzomyia (Lu.) ayacuchensis* salivary glands. The deduced amino acid sequences are shown by the single-letter amino acid code under the nucleotide sequences. The putative signal peptide is underlined. (B) Sequence alignment of mature RGD-containing peptides identified from salivary glands of *Lu. ayacuchensis* (ayadualin), *Lu. longipalpis* (LuloRGD), and *Lu. intermedia* (Linb-1 and Linb-2). Black and grey-shaded amino acids represent identical and conserved residues, respectively. Asterisks denote RGD (Arg-Gly-Asp) sequences, and closed circles indicate cysteine residues.

Fig. 2. SDS-PAGE analysis of recombinant ayadualin and ΔRGD, and a CS mutant expressed in *Escherichia coli*. *Escherichia coli* was transformed with ayadualin, ΔRGD or a CS mutant-expressing plasmid vector, and expression of the Trx-His-tagged recombinant proteins was induced by IPTG. Recombinant proteins, Trx-His-ayadualin (lane 2), Trx-His-ayadualin ΔRGD (lane 3) or Trx-His-ayadualin CS mutant (lane 4) were purified from the soluble fraction and subjected to SDS-PAGE analysis. Trx-His-tag protein only was expressed and purified for use as a control (lane 1). Lane M, protein molecular weight marker.

Fig. 3. Inhibition of collagen and ADP- induced platelet aggregation by ayadualin. Platelet rich plasma was mixed with ayadualin (■), ΔRGD (▲), CS mutant (▼), or Trx-His-tag protein (●) with the final concentration of 20, 10, 5, 2.5, 1.25 or 0.625 μM,

and platelet aggregation was induced immediately by addition of collagen (A) or ADP (B). Platelet aggregation was measured by determining the change in light transmission at a wavelength of 630 nm. The results are expressed as the mean for triplicate assays ± standard deviation.

Fig. 4. Inhibition of binding of integrin $\alpha_{IIb}\beta_3$ to immobilized fibrinogen by ayadualin. Inhibition of fibrinogen/integrin $\alpha_{IIb}\beta_3$ (GPIIb-IIIa) was measured by a solid-phase ELISA. Serially diluted ayadualin (■), ΔRGD (▲), CS mutant (▼), or Trx-His-tag protein (●) was added to the fibrinogen-coated wells with the final concentration of 0.8, 0.16, 0.032 or 0.0064 μM, followed immediately by addition of purified human integrin $\alpha_{IIb}\beta_3$ (GPIIb-IIIa). The binding of integrin $\alpha_{IIb}\beta_3$ to fibrinogen was detected by an anti-CD41 (GPIIb) monoclonal antibody and expressed as percent binding relative to wells containing Trx-His-tag protein and integrin $\alpha_{IIb}\beta_3$. The results are expressed as the mean for triplicate assays ± standard deviation.

Fig. 5. Inhibition of intrinsic coagulation by recombinant ayadualin. The inhibitory effect of ayadualin on the intrinsic coagulation pathway was examined using the activated partial thromboplastin time (APTT) assay. Citrated human plasma was incubated with ayadualin (■), ΔRGD (▲) or Trx-His-tag protein (●), and activated with APTT reagent. Clot formation was measured using a coagulometer. The results are expressed as the mean for triplicate assays ± standard deviation.

Fig. 6. Inhibitory effects of ayadualin on the enzymatic activity of kallikrein, FXIIa, FIXa, and FXa. Citrated human plasma was incubated with various concentrations of

ayadualin (■) or Trx-His-tag protein (●), and activated with APTT reagent. The generated kallikrein (A), FXIIa (B), FIXa (C), and FXa (D) activities were measured using chromogenic substrates. The results are expressed as the mean for triplicate assays ± standard deviation.

Fig. 7. Inhibitory effect of ayadualin on FXII. FXII was treated with ayadualin (■) or Trx-His-tag protein (●) before (A) or after (B) activation, and enzymatic activity of FXIIa was measured. The results are expressed as the mean for triplicate assays ± standard deviation.

Fig. S1. Phylogenetic tree analysis of RGD-containing peptides. The sequences of ayadualin along with those of RGD-containing peptides were aligned, and phylogenetic analysis was performed. The GenBank accession numbers of the proteins used for this analysis are as follows: albolabrin (P62384), barbourin (P22827), dendroaspin (2104176A), echistatin (AAA72777), elegantin 2a (AAB50832), flavoridin (1FVL_A), kistrin (1N4Y_A), trigramin (P17495), decorsin (P17350), ixodegrins (AAT92147), monogrin 1A, B (ABI52649, ABI52650), savignygrin (AAM54048), tabinhibitin3-7 (ACS72293-ACS72297), LuloRGD (AAD32196), Linb-1, 2(AFP99227, AFP99242). The scale bar represents 0.2 % divergence.

Fig. S2. Amino acid sequences of ayadualin, ΔRGD, and CS mutant.

Fig. S3. Effect of ayadualin on FXa and kallikrein activity in FXII-deficient plasma. FXII-deficient plasma was incubated with ayadualin (■) or Trx-His-tag protein (□), and activated by FXIIa. The generated FIXa and kallikrein activities were measured using chromogenic substrates. The results are expressed as the mean for triplicate assays ± standard deviation.

A

```
CGGCCTTACGGCCGGGGGTTAGTCAGTTGTGGAAATTACCTGCAAAATGAATAAGATTAT   60
                                                M  N  K  I  I    5

TCTATTTTCTGCTGTTTTTCTGGCATTAGTGTTTTGTGCTGAGGCCATGCCAAGGGAAAG  120
  L  F  S  A  V  F  L  A  L  V  F  C  A  E  A  M  P  R  E  S   25

CGTAAATATTCTCAATGCTGAAAATGAACCTGACGACACCGTGGACATAGATGAGGGTCT  180
  V  N  I  L  N  A  E  N  E  P  D  D  T  V  D  I  D  E  G  L   45

TCCTGATGCATTCGACGAGGATTATGAACAGGATGGTCATAATCCATATCCCTGTAGAGG  240
  P  D  A  F  D  E  D  Y  E  Q  D  G  H  N  P  Y  P  C  R  G   65

AGACTGCTAGTAAACTGACATTCTACTGACTATTCAGCTAACCAAAAATATGTAAAATTT  300
  D  C  *                                                       67

AAATGTATCTGAAGCTGTTTATAAGACGAACATCATGGAATAATAAACTTTCACTCAGCA  360

ATAAAAAAAAAAAAAAAAAAAA                                        382
```

B

```
                                                          •***•
ayadualin MPR-E--SVNILNAENEPDD--------TVDIDEGLPDAFDEDYE-QDGHNPYPCRGDC--- 47
LuloRGD   MEATEEISVKLQDDANEPDD--------SLDLDEGLPDAFDEDYNNQAEYKPNP-RGDYRRR 53
Linb-1    MPK-D--VAEVELLDEDLSDMDIDKLVDQIQIDEDTP------YE-AELPCNNP-RGDC--- 48
Linb-2    MPK-E--QIHVNVLDEEA-DN-------KVDIDEDIP------YEFSDKPCNNP-RGDC--- 41
                                                       •          •
```

Fig. 1

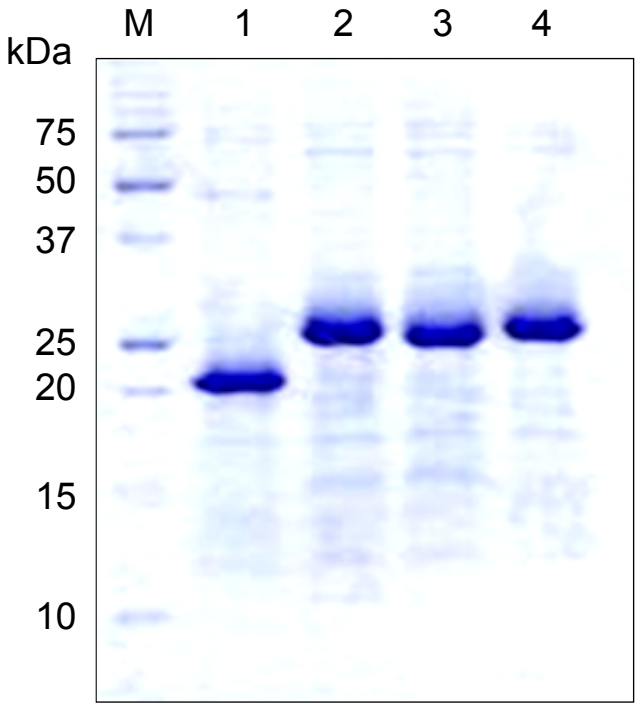

Fig. 2

A

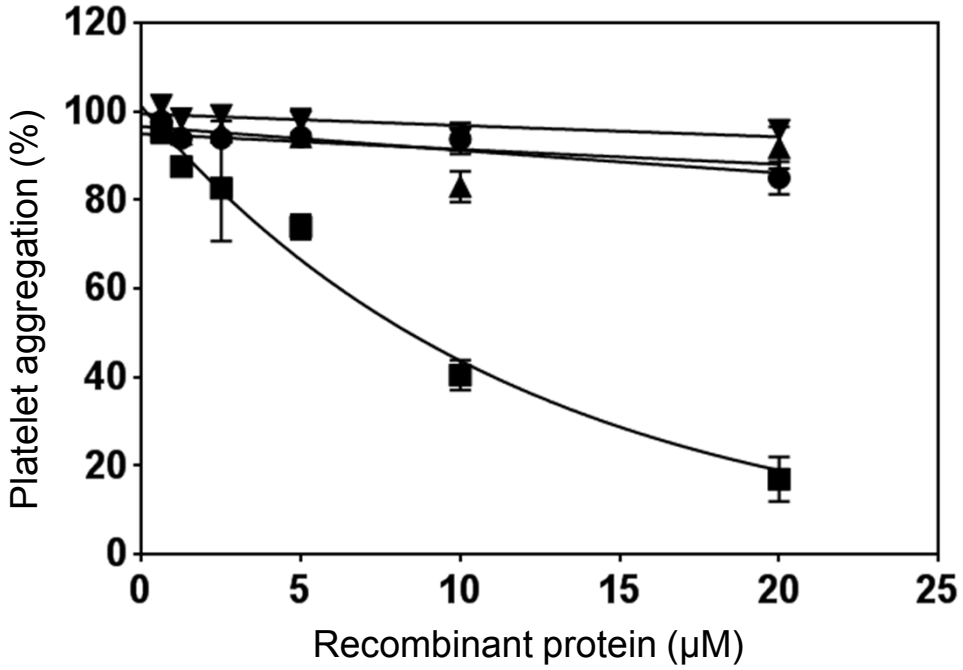
120
100
80
60
40
20
0
Platelet aggregation (%)
0
5
10
15
20
25
Recombinant protein (μM)

B

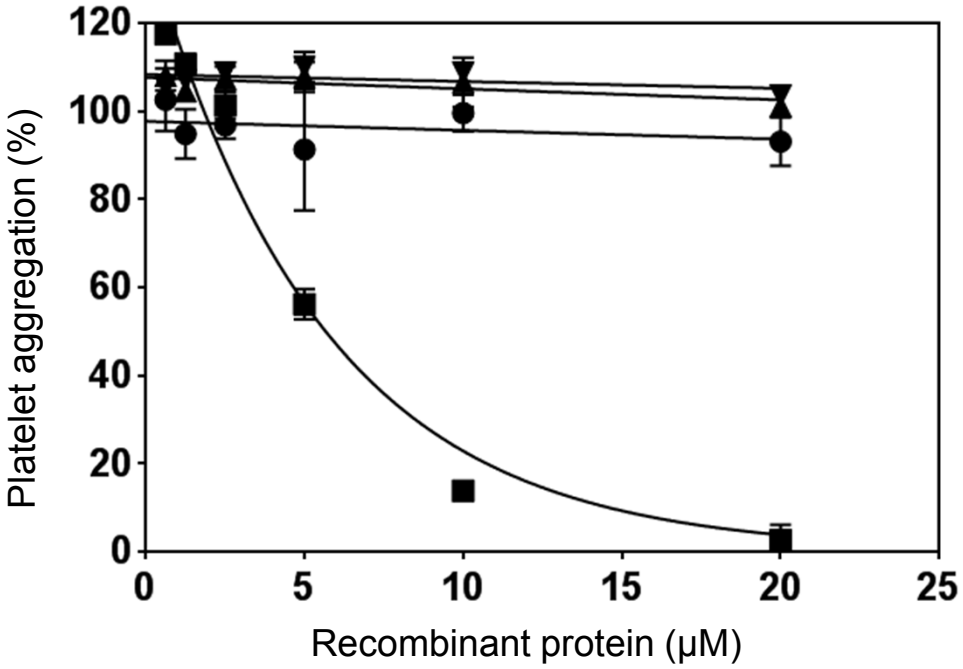
120
100
80
60
40
20
0
Platelet aggregation (%)
0
5
10
15
20
25
Recombinant protein (μM)

Fig. 3

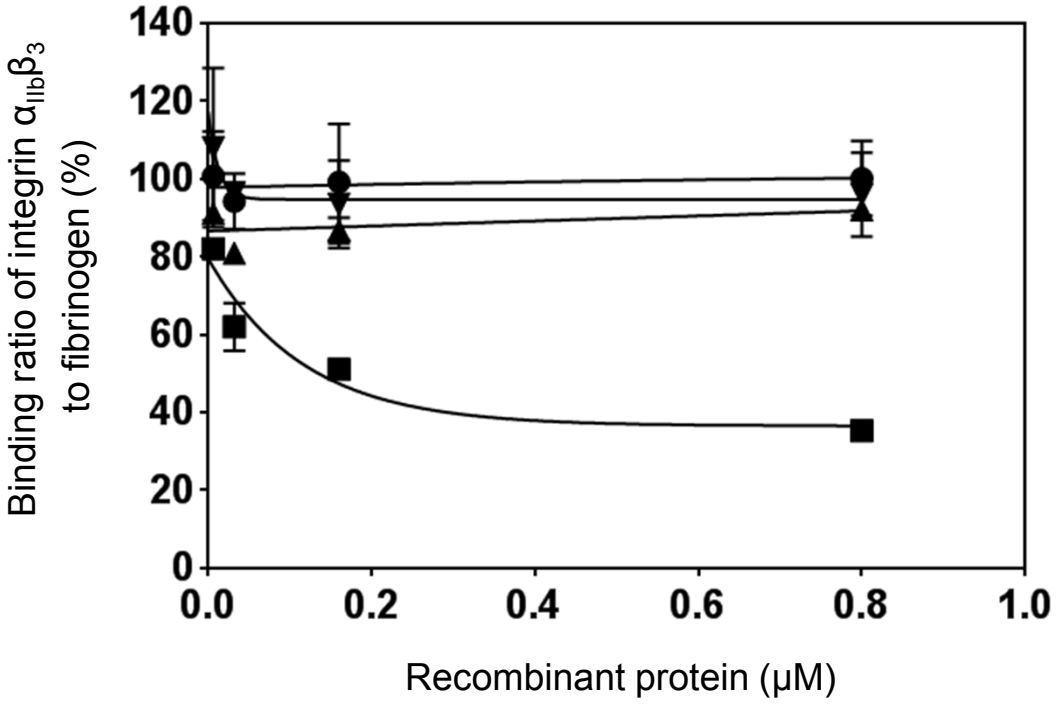
Binding ratio of integrin $\alpha_{IIb}\beta_3$ to fibrinogen (%)
140
120
100
80
60
40
20
0
0.0
0.2
0.4
0.6
0.8
1.0
Recombinant protein (μM)

Fig. 4

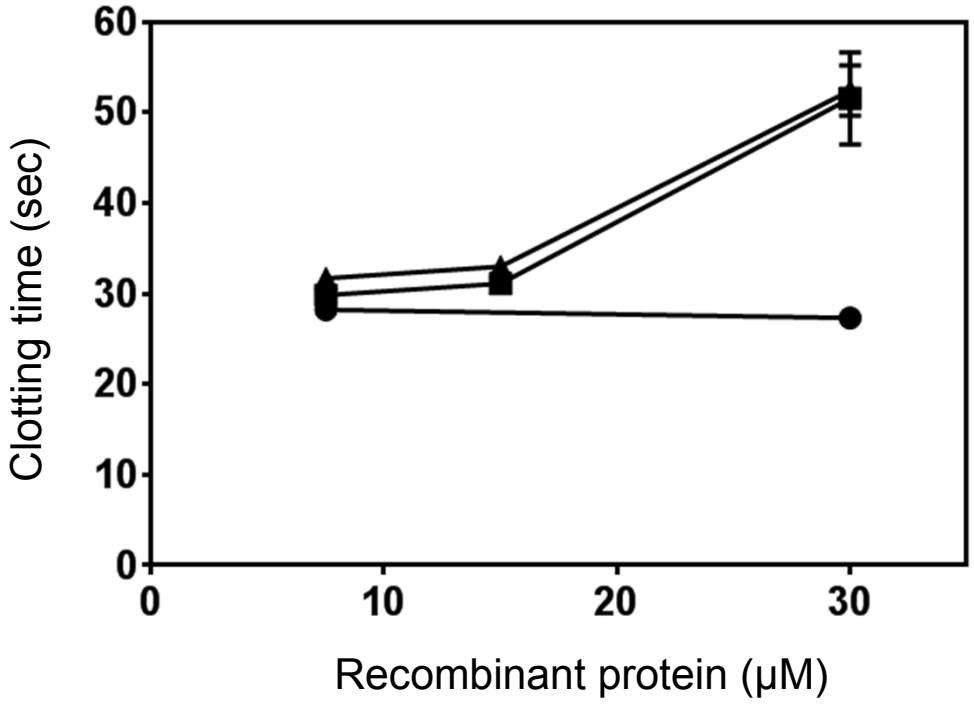
60
50
40
30
20
10
0
Clotting time (sec)
0
10
20
30
Recombinant protein (μM)

Fig. 5

A

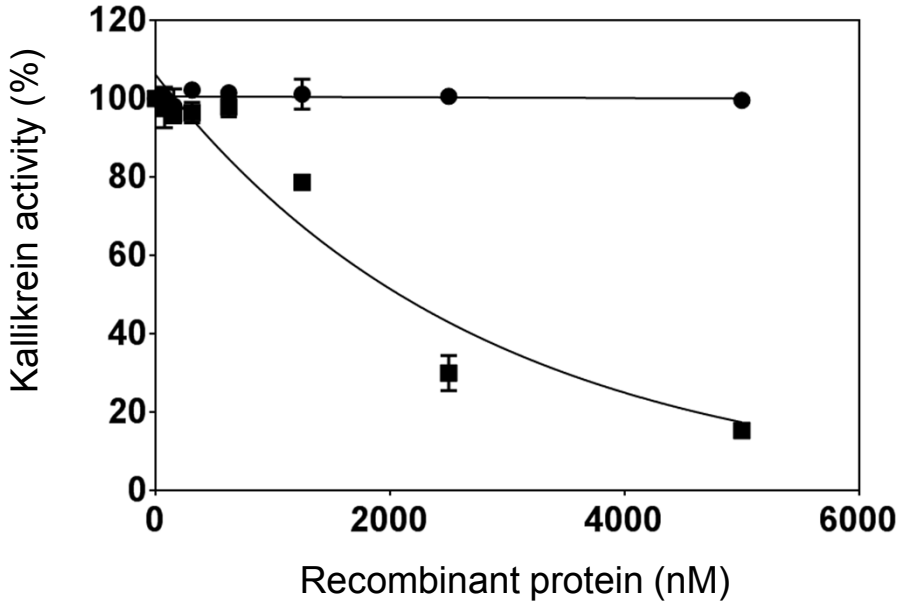
Kallikrein activity (%)
120
100
80
60
40
20
0
0
2000
4000
6000
Recombinant protein (nM)

B

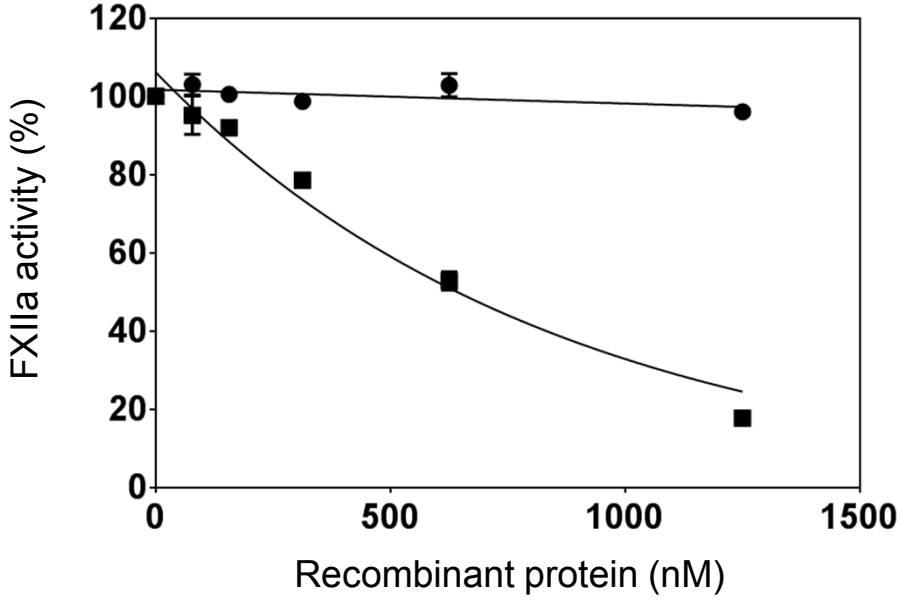
FXIIa activity (%)
120
100
80
60
40
20
0
0
500
1000
1500
Recombinant protein (nM)

Fig. 6

C

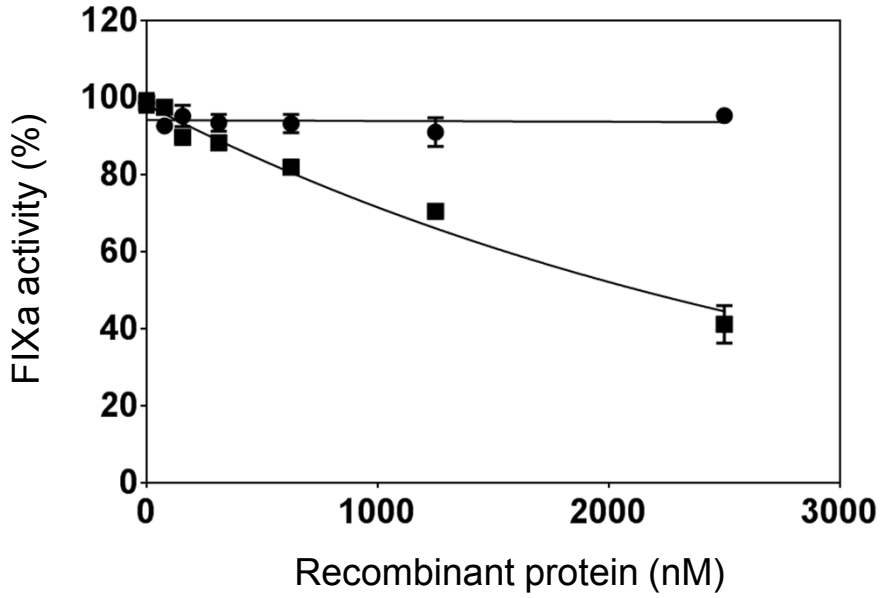
120
100
80
60
40
20
0
FIXa activity (%)
0
1000
2000
3000
Recombinant protein (nM)

D

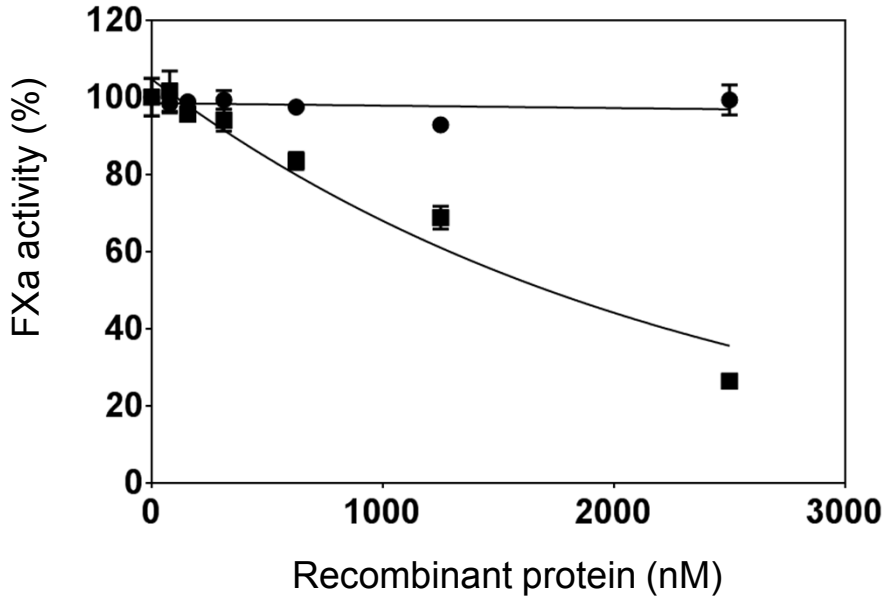
120
100
80
60
40
20
0
FXa activity (%)
0
1000
2000
3000
Recombinant protein (nM)

Fig. 6

A

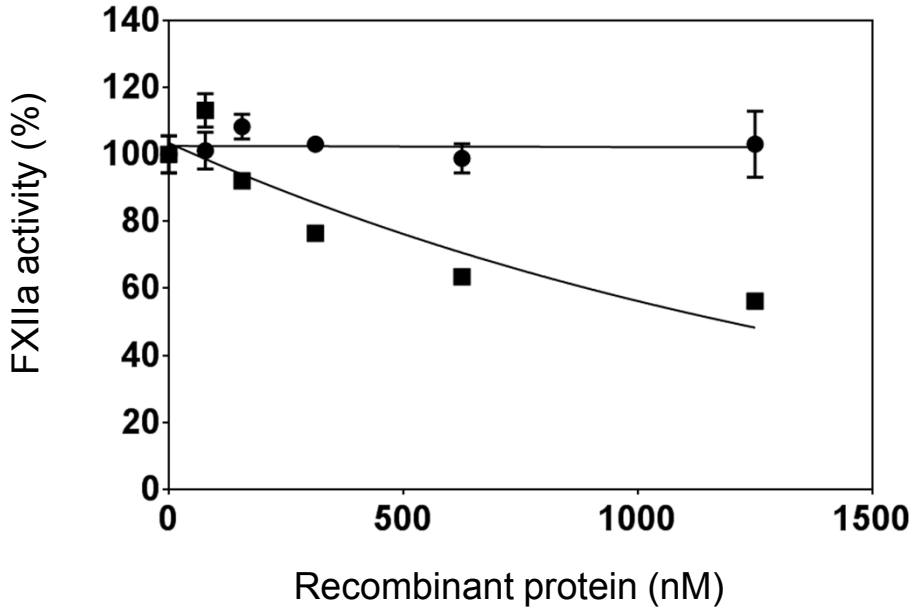
140
120
100
80
60
40
20
0
FXIIa activity (%)
0
500
1000
1500
Recombinant protein (nM)

B

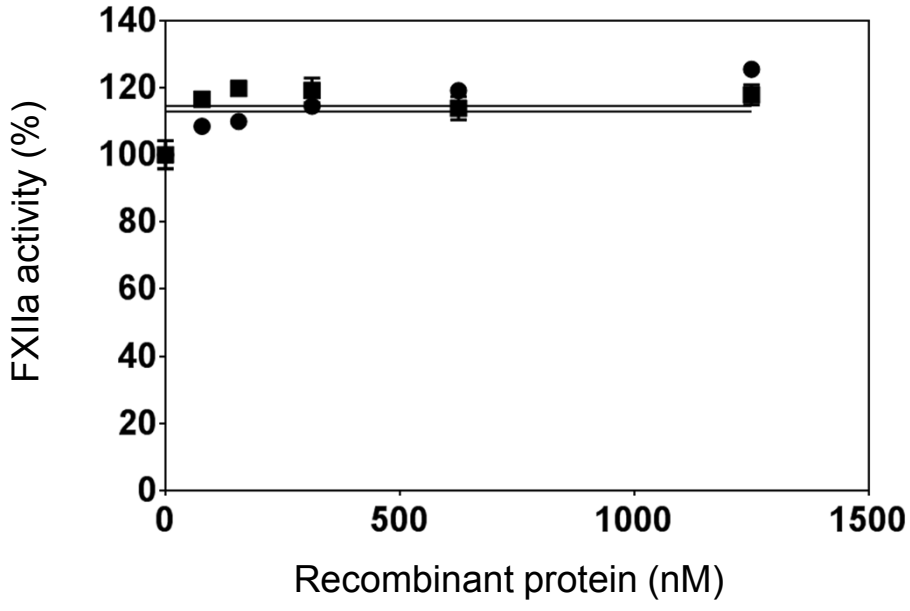
140
120
100
80
60
40
20
0
FXIIa activity (%)
0
500
1000
1500
Recombinant protein (nM)

Fig. 7